An inertial tribometer for measuring microslip dissipation at a solid–solid multicontact interface

Tristan Baumberger, Lionel Bureau, Michel Busson, Eric Falcon, and Bernard Perrin
Laboratoire de Physique de la Matière Condensée,[a] Ecole Normale supérieure, 24 rue Lhomond, 75231 Paris Cedex 05, France

(Received 17 November 1997; accepted for publication 5 March 1998)

An apparatus has been built to measure the shear response of a multicontact interface between flat-ended solid bodies, rough at the micron scale. The device makes use of inertia to apply a steady sinusoidal shear force to a slider without direct mechanical drive. Both elastic compliance and damping losses are deduced from the in-phase and out-of-phase components of the submicronic shear displacement. Operating frequencies range between 15 Hz and 1 kHz, while below 100 Hz quasistatic motion of the slider is achieved. Acceleration amplitudes range typically between 0.1 and 7 m s^{-2}, where gross sliding occurs. The resolution of the microslip detection is 1 nm. Apparatus design and operation are described, and the application and limitation of the method to a weakly nonlinear response are discussed and illustrated by experimental results with a polymer glass. © *1998 American Institute of Physics.* [S0034-6748(98)00406-7]

I. INTRODUCTION

In recent years, the *multicontact interface* between nominally flat surfaces, though microscopically rough, has aroused sustained interest as a model system for the study of sliding friction.[1,2] Consisting of a large number of microcontacts, far enough from each other to be considered as elastically independent, such an interface shows original tribological properties which are relevant to the mechanics of a single contact, as well as to the statistical physics of a junction set. A standard configuration involves a slider driven along a track by way of a translation stage of finite compliance. The resulting dynamics, featuring stick-slip oscillations, has been adequately described by a phenomenological state- and rate-dependent friction force.[1] The underlying physical mechanisms remain, however, widely unknown, especially regarding the microscopic origin of the dissipative process giving rise to macroscopic solid friction. It is therefore of fundamental interest to probe the shear resistance of a multicontact interface prior to gross sliding, in a macroscopic *stick* phase which reveals microscopic relative motion, referred to as *microslip*.

A. Previous work in the field

In the past, microslip has been extensively studied in configurations involving a single contact patch of size typically 100 μm, e.g., between a steel sphere and a steel flat, submitted to an oscillating shear force.[3–5] Dealing with a multicontact interface raises rather stringent constraints and requires original solutions. Typical surfaces used in multicontact experiments have a roughness of order 1 μm and an area of 1×1 cm^2. The maximum micro-slip that the interface can sustain before gross sliding is also on the order of microns, presumably scaling with the mean size of the microcontact population. According to these length scales, the apparatus should conveniently enable measuring submicron displacements while preventing tilt and misalignment of surfaces higher than (1 μm)/(1 cm) $\simeq 10^{-4}$ rad. Moreover, applying an alternate shear force to the slider requires a push–pull mechanism which is likely to show some play. Olofsson[6,7] has carried out experiments on various materials using a servo-hydraulic tension–torsion machine. The study was restricted to very low frequencies (typically 10^{-2} Hz), a serious drawback when working with materials showing significant creep aging—such as glassy polymers,[1,2] which may affect the strength of the interface during one cycle.

B. Principle of the inertial tribometer

The tribometer developed uses an alternative way of applying a shear force to the slider without direct mechanical drive. The track itself is moved back and forth so that, within the framework attached to the latter, the slider is submitted to an inertial shear force acting on its center of mass G. The relative displacement x of the slider with respect to the track is measured, together with the acceleration γg of the track itself, with g$\simeq$9.8 m s^{-2} the acceleration of gravity. The track being horizontal, the normal load is provided by the weight mg of the slider. The equation of relative motion of the slider is thus:

$$m\frac{d^2x}{dt^2} = -mg\gamma + F, \tag{1}$$

where F is the shear interfacial resistance. In a typical experiment the input is $\gamma(t)$ the track acceleration in unit g, and the output shall be the force-displacement characteristics F—x. The left-hand term is therefore troublesome inasmuch as it must be evaluated by differentiating twice the measured $x(t)$, a highly noise-sensitive process. When this term is negligible, the relative motion of the slider is quasistatic and the

[a]Associated with: Centre National de la Recherche Scientifique et aux Universités Paris 6 et Paris 7.

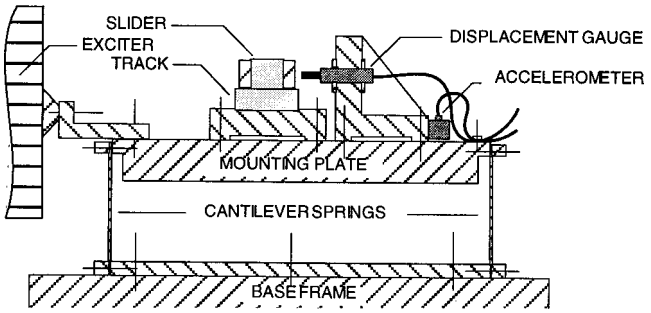

FIG. 1. Overall diagram of the inertial tribometer. The total height of the apparatus over the base frame is 17 cm; its total length is 25 cm. The vibration exciter is fixed with respect to the base frame (not shown).

shear resistance F is just γmg. The frequency limit of the quasistatic regime will be specified in Sec. III A 2.

A typical experiment consists of applying a sinusoidal γ at a frequency f and measuring the components of the slider displacement at f, in-phase (x_0) and out-of-phase (x_{90}) with the excitation γ.

II. DESCRIPTION AND DESIGN OF THE INERTIAL TRIBOMETER

A. Mechanical arrangement

A schematic drawing of the apparatus is shown in Fig. 1. The physical object dealt within the study, the multicontact interface, is located between two samples—the preparation of which is described in Sec. II C. The lower sample, referred to as the track, is glued with Araldite on a 20 mm thick duralumin piece which itself is clamped on a 30 mm thick duralumin mounting plate. The upper sample, a 20 mm cube, is fixed into a duralumin holder—referred to as the slider, which is sketched Fig. 2. The slider includes two brass counterweights hanging sideways and whose vertical level can be adjusted in order to locate the center of mass G of the slider at the interface. The total mass of the slider is $m=230$ g for a sample made of poly(methyl methacrylate) (PMMA). The track mounting plate is fixed to the massive base frame by a double cantilever-spring flexure system, 100 mm high, which ensures the translation motion of the plate. The oscillating drive is provided by an electromagnetic vibration exciter (BRÜEL & KJÆR, type 4809). The exciter is attached to the base frame through a three-axes positioner and can thus be aligned precisely with the mounting plate. The coupling is ensured by a duralumin piece. The relative displacement x of the slider is measured by an eddy-current linear displacement gauge (ELECTRO, sensor 4937, module PBA200). The gauge sensor is attached to a massive holder clamped to the mounting plate. The end of the sensor is located 1 mm ahead of the slider and performs remote gauging. The acceleration γg of the mounting plate is measured with a piezoelectric accelerometer (BRÜEL & KJÆR, type 4371 V) glued with cyanocrylate adhesive to the gauge holder.

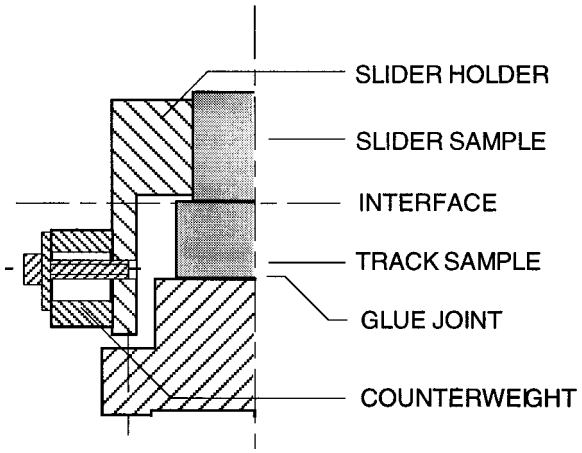

FIG. 2. Half cross-sectional detail of the slider, showing one of the adjustable counterweights which allow the center of mass of the slider to be located at the slider-track interface.

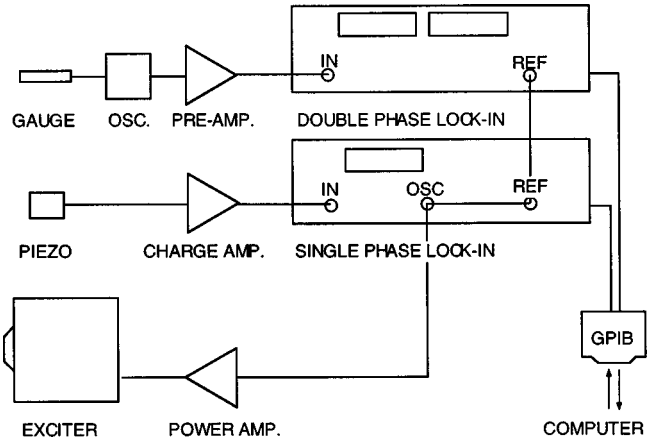

FIG. 3. Block diagram of the excitation-detection system.

B. Excitation and detection systems

The system is sketched in Fig. 3. The analog signals proportional to $x(t)$ and $\gamma(t)$ are sent to two lock-in amplifiers. The internal reference provided by the oscillator of one of the amplifiers is used as a reference for the second one. It is also power-amplified to feed the exciter.

The acceleration signal is provided by a charge amplifier whose gain is set according to the calibration chart of the accelerometer head.[8] The output sensitivity is 0.1 V m^{-1} s^2.

The output signal of the oscillating circuit including the displacement inductive gauge consists of a dc bias which grows in proportion to the probe-target distance, and a residual ac component at about 300 kHz—the frequency of the built-in oscillator. The signal is notch-filtered to remove most of the ac component, then preamplified by a custom-made, op-amp based circuit. The overall sensitivity, 0.55 V μm^{-1}, is determined by the following calibration procedure. The inductive sensor, fixed in a holder attached to the base frame, probes the motion of the mounting plate, oscillating at a frequency chosen within the operating range. The amplitude of oscillation is directly determined by the accelerometer, whose charge signal is integrated twice—an analog facility of the charge amplifier. The sensitivity has been checked to be frequency-independent within the operating range. The linearity error over a 1 μm displacement is 3%.

The measured signals are the components of the relative displacement of the slider, in-phase (x_0) and out-of-phase

(x_{90}) with respect to γ, the acceleration of the track in unit g. A careful synchronization of the displacement and the acceleration is therefore required. The procedure adopted in this study consists of setting to zero the phase shifts of the lock-in amplifiers when using a very low amplitude of excitation, namely 0.02 g, at which the response of the interface is supposed to be mostly elastic, and therefore in-phase with the acceleration. We come back to this point in Sec. IV.

C. Sample preparation

The inertial tribometer has been designed to study the shear properties of a multicontact interface between two flat-ended rough bodies. A typical roughness is 1 μm rms and it is essential for the sake of homogeneity of the microcontact population that surfaces have a flatness better than 1 μm. This is usually obtained by grinding face-to-face the slider and the track. Due to the size of the samples, an alternative procedure has been used. Each sample is fixed to the piston of a grinding-chuck and hand-lapped against a reference flat, namely a float-glass plate, with SiC 23 μm powder (Grit#400) in a water-soluble lubricant. Starting from good quality surfaces (e.g., optically flat polymer glass or rectified aluminum alloy) the surface finish is characterized by a rms roughness of 1.3 μm, as measured over a 400×400 μm sample zone with an three-dimensional interferometric profilometer. The resulting interface is found to fulfill the conformation requirement, inasmuch as the slider shows neither significant tilt nor spin under shear, as described in Sec. III B 3.

III. OPERATING LIMITATIONS, UNCERTAINTIES AND BIAS

In this section, the characteristics of the inertial tribometer are illustrated by experimental results obtained with an interface between samples of PMMA prepared as described in Sec. II C.

A. Frequency limitations

1. Low frequency limitations

A low frequency limitation arises from the maximum displacement of the exciter, namely 8 mm peak-to-peak. The maximum acceleration that the slider can sustain before sliding is given by μ_sg where μ_s is the static friction coefficient. For a conservative value, $\mu_s \simeq 0.6$, the minimum frequency allowing the full acceleration range to be used is therefore 6 Hz. At this frequency, however, the response of the accelerometer is shifted by typically 2°.[8] Since the acceleration signal is used as a reference, and since the loss angle, $\arctan(x_{90}/x_0)$, remains typically smaller than 6°, such a phase shift would affect significantly the out-of-phase component of the displacement x_{90}; therefore, we have restricted the operating frequencies to above 15 Hz where the phase shift is nominally zero.

2. High frequency limitations

A high frequency limit arises from the phase shift of the accelerometer which becomes significant above 1 kHz, and from the resonance of the flexural modes of the cantilever springs, the first one being 670 Hz. The latter can be removed, however, by sticking a pad of plasticine on the springs. In practice, the frequency range is even narrower, due to the quasistatic requirement evoked in Sec. I B, which prohibits high frequencies for which the relative acceleration of the slider becomes higher than the absolute acceleration of the track. In order to estimate the upper frequency limit, the interface is supposed to be perfectly elastic and linear, with a stiffness κ. The amplitudes of both acceleration terms, namely $\omega^2 x^{\max}$ and $\gamma^{\max}$g are then related according to:

$$\omega^2 x^{\max} = \frac{\gamma^{\max} g}{|1-(\omega_0/\omega)^2|}, \tag{2}$$

where $\omega = 2\pi f$ and $\omega_0 = \sqrt{\kappa/m}$, the eigen pulsation of the system interface/slider. The quasistatic approximation therefore requires $\omega \ll \omega_0$. A previous study[9] has shown the proportionality between the shear stiffness of a multicontact interface and the normal load (here mg): $\kappa = mg/\lambda$, where λ is a length typically of micron order. Hence, the eigen pulsation value of the system is determined by: $\omega_0 = \sqrt{g/\lambda}$, independent of the mass. This resonant shear mode is clearly seen in Fig. 4 about 470 Hz. For the relative acceleration of the slider to remain less than 5% of the absolute acceleration of the track, the frequency should remain below 100 Hz.

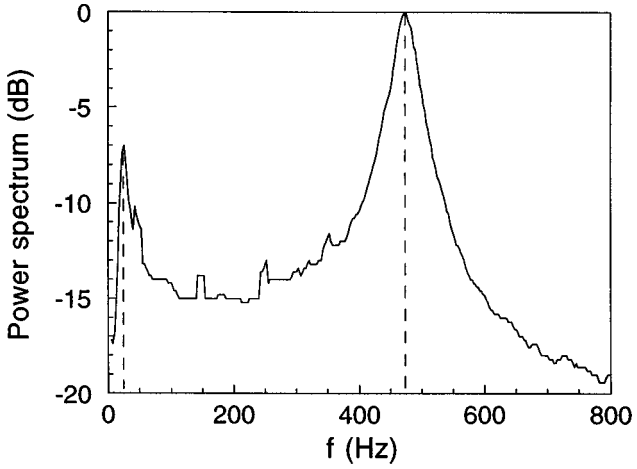

FIG. 4. Spectral response of the slider relative displacement, when a random noise is sent at the input of the exciter, resulting in a rms acceleration of 0.01 g. The peak at 25 Hz is the resonance of the vibration stage (double cantilever spring-mounting plate); the peak at 470 Hz is the resonance of the slider-track interfacial shear mode.

3. Resonance of the excitation stage

The phase of the acceleration signal, once set to zero at low excitation, remains null within 0.4° over the operating range of acceleration, at all frequencies except in the close vicinity of the main resonance of the system—including the double cantilever-spring, the mounting plate, the slider, and the exciter—where the phase shift can reach a few degrees. This is shown in Fig. 5 where the out-of-phase displacement x_{90} is plotted with respect to frequency, while the excitation amplitude remains fixed. It is found to be frequency-independent, except for a sharp artefact about 25 Hz which closely matches the resonance peak of the system (Fig. 4).

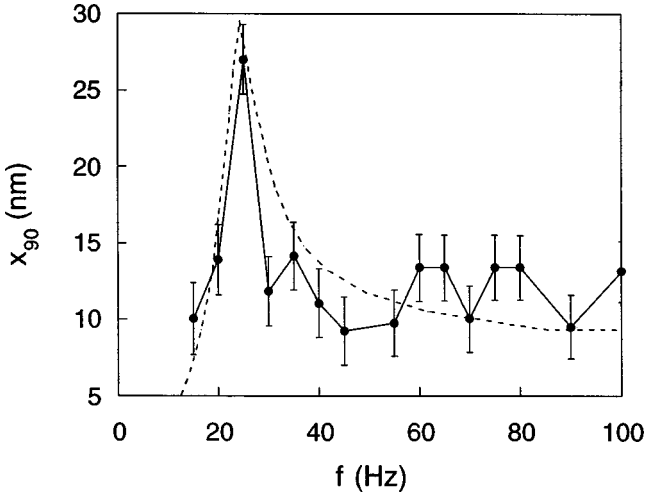

FIG. 5. Out-of-phase response (dots) of the slider x_{90} to a shear force at frequency f, while keeping the maximum acceleration fixed to 0.3 g. The sharp artefact about 25 Hz corresponds to the resonance of the vibration stage whose line shape (dashed line) is displayed in arbitrary units. The error bars correspond to uncertainty on the reference phase (see the text for details).

This unexpected bias is attributed to the enhanced sensitivity of the system to even weakly nonlinear components—the principle one being the interface itself—which may result in complex amplitude-phase coupling at resonance.

Ultimately, the operating frequency range for the reported mechanical and electronic configuration is 15–100 Hz with a ± 5 Hz notch about 25 Hz. This range can be extended up to kHz for the purpose of the spectral response analysis.

B. Unwanted forces and displacements

1. Vertical acceleration

The double cantilever attachment ensures that the mounting plate oscillates parallel to itself. However, there remains a small overall vertical motion. A straightforward geometric estimation of the corresponding acceleration yields 6×10^{-2} m s^{-2} as an upper boundary over the whole range of horizontal acceleration of the table. This results in a modulation of the weight of the slider by less than 1%.

2. Structure compliance

The principle of the tribometer, which is to obtain interfacial data from remote displacement gauging, requires that the compliance of the mounting plate including the clamped track and gauge holders remain smaller than the compliance of the interface itself. This has been checked by measuring the relative displacements of both the track and the slider with respect to the gauge holder, using two identical heads, sensing above and below the interface, respectively. The spurious relative displacement (Fig. 6) is found to remain smaller than 5% of the displacement x at all frequencies. In this respect, it was important to build the apparatus with massive stands and to take special care with the clamped joints. These were restricted to relatively small raised surfaces, lightly roughened by lapping.

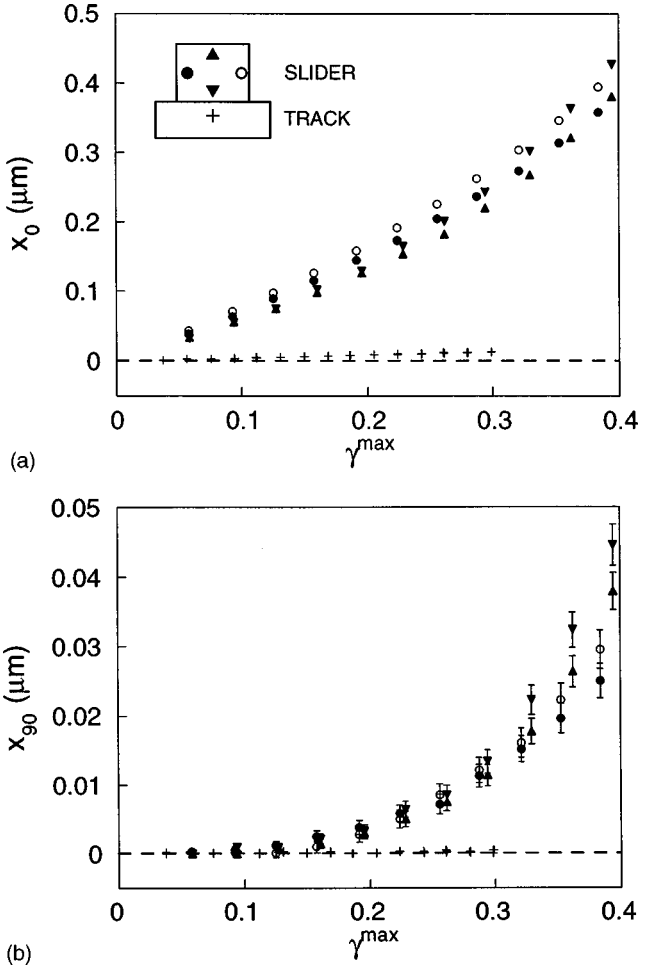

FIG. 6. Scaled output of the displacement gauge with respect to the maximum acceleration in unit g, at 40 Hz, for different sensing positions. (a) In-phase component x_0. The sensing positions are located on a schematic front view of the slider-track system. (b) Out-of-phase component x_{90} with error bars as in Fig. 5.

3. Tilt and spin of the slider

Careful location of the center of mass of the slider within the interface is a prerequisite to any experiment with a newly mounted sample. First, the counterweights are approximately located at a level calculated from the knowledge of the geometry of the slider. Then, a control experiment is performed with the slider on the oscillating track, while its relative displacements are measured by two identical position sensors—the first one sensing the bottom of the slider and the second one being located close to the top 2 cm above. A fine adjustment of the level of the counterweights enables both displacement signals to be equalized. A typical result is shown in Fig. 6 for both the in-phase and out-of-phase components. From these data, it may be inferred that the tilt of the slider remains smaller than 2×10^{-6} rad.

Nonhomogeneous lapping of the surfaces in contact results in the spin of the slider about a vertical axis. This is checked using two displacement gauges located at the same horizontal level but sensing, respectively, a right- and a left-hand front part of the slider, separated by 2 cm. The displacements are shown in Fig. 6. Here too, a conservative upper bound to the spin angle is 2×10^{-6} rad.

C. Resolution and uncertainty on the out-of-phase, dissipative component

The main source of scattering of the experimental data for x_{90}, when working with a fixed set of microcontacts, remains the uncertainty on the reference phase $\Delta\phi \simeq 0.4°$, i.e., 7×10^{-3} rad. The resulting uncertainty on x_{90} is therefore $\Delta x_{90} \simeq x_0 \Delta\phi$. This is displayed as error bars on Figs. 5 and 6(b).

The ultimate resolution for x_{90} is 1 nm. As mentioned in the Appendix, x_{90} is related directly to the energy losses associated with interfacial damping. The apparatus enables the onset and development of dissipation, precursory to full sliding friction, to be investigated between typically 0.1 and 10 μJ/cycle.

IV. DISCUSSION AND PROSPECTS

The inertial tribometer described in this article has been developed for the study of the microslip energy dissipation under unlubricated conditions, at a multicontact interface between surfaces having cm^2 apparent contact area and μm roughness, showing an interfacial elastic shear mode with a resonance frequency about 500 Hz. The whole apparatus has been designed and scaled according to these figures but can be adapted as well to other interfacial problems for which remote loading and sensing are required. In particular, the exciter we have used is a small one, with maximum force rating 45 N. It is oversized for the purpose of using larger and heavier samples, or studying the system in a special environment, e.g., in a temperature or atmosphere-controlled box.

The efficiency of the method has been illustrated using a polymer glass, but tests performed on an aluminum alloy display qualitatively similar results. It should be kept in mind, however, that the synchronization procedure described in Sec. II B assumes that there is no finite phase shift as the force amplitude tends to zero, as expected for frictional dissipation. It therefore removes from x_{90} any viscoelastic loss in the sheared asperity while retaining the interfacial microslip contribution. Such internal loss, negligible for the aluminum alloy, is expected to be significant when using a polymer glass and its measurement requires an absolute synchronization of the displacement signal with the acceleration one: The slider is removed from the sensing zone and replaced by a metallic target, fixed with respect to the base frame; the mounting table is then vibrated and the phase reference of the displacement gauge amplifier is set to zero, since the displacement and the acceleration are then ensured to be in-phase. This phase reference is kept fixed while operating at a prescribed frequency. Any change in frequency requires one to repeat the synchronization procedure to account for frequency-dependent phase shift along the mechanical and electrical circuits. This heavier procedure is found to be strictly equivalent to the one described in Sec. II B when working with the aluminum alloy. When using the polymer glass, it is found that x_{90}/x_0 tends to a finite value $\tan\delta \simeq 0.1$ as γ vanishes. The value for δ is compatible with the loss angle of the bulk material at the operating frequency.

At this stage of development, the main limit of the apparatus arises when dealing with *nonlinear* response, such as displayed in Fig. 6. As detailed in the Appendix, the in-phase component x_0 is then no longer a straightforward, quantitative characteristic of the interfacial strength. This problem can be overcome by biasing the interface with a dc-shear force, provided by tilting the whole setup with respect to the vertical axis, while remaining within the ''friction cone'': for a static friction coefficient $\mu_s = 0.6$, the maximum tilt angle is thus $\arctan(\mu_s) \simeq 31°$. A small inertial ac-shear force can then be superimposed, as described in the text, in order to probe locally the $F-x$ characteristics of the interface.

APPENDIX: ON THE MEANING OF THE MEASUREMENTS FOR A NONLINEAR RESPONSE

The in-phase and out-of-phase components of the relative displacement, as provided by a lock-in amplifier synchronous with the zero-biased external force $F(t) = F^{\max}\cos(\omega t)$, are calculated according to:

$$x_0 = \frac{\omega}{\pi}\int_{-\pi/\omega}^{+\pi/\omega} x(t)\cos(\omega t)\,dt, \tag{A1}$$

$$x_{90} = \frac{\omega}{\pi}\int_{-\pi/\omega}^{+\pi/\omega} x(t)\sin(\omega t)\,dt. \tag{A2}$$

For a linear response $x(t) = x_0^{\max}\cos(\omega t) + x_{90}^{\max}\sin(\omega t)$, it is clear that $x_0 = x_0^{\max}$ and $x_{90} = x_{90}^{\max}$. In particular, the interfacial elastic stiffness is

$$\kappa = \frac{dF}{dx} = \frac{F^{\max}}{x_0}, \tag{A3}$$

and the steady-state energy losses per cycle are given by

$$E = \oint F\,dx = \pi F^{\max} x_{90}. \tag{A4}$$

When the response is nonlinear, Eq. (A4) holds as long as the applied force has no higher harmonics. Hence, the meaning of x_{90} as a characteristic of the interfacial damping is preserved. The in-phase displacement x_0 is now just the amplitude of the first harmonic, in phase with the shear force. It therefore has no simple quantitative meaning with regard to the shear elasticity of the interface. However, for a weakly nonlinear response, the evolution of $F^{\max}/x_0$ with $F^{\max}$ may indicate the *trend* towards either weakening or strengthening of the interfacial stiffness.

[1] T. Baumberger, Solid State Commun. **102**, 175 (1997).
[2] J. H. Dieterich and B. D. Kilgore, Pure Appl. Geophys. **143**, 283 (1994).
[3] R. D. Mindlin, W. P. Mason, T. F. Osmer, and H. Deresiewicz, *Proceedings of the 1st US National Congress of Applied Mechanics* (ASME, New York, 1952), pp. 203–208.
[4] K. L. Johnson, Proc. R. Soc. London, Ser. A **230**, 531 (1955).
[5] L. E. Goodman and C. B. Brown, Trans. ASME, J. Appl. Mech. **29**, 17 (1962).
[6] U. Olofsson and M. Holmgren, Exp. Mech. **34**, 202 (1994).
[7] U. Olofsson, Tribol. Int. **28**, 207 (1995).
[8] BRÜEL & KJÆR, Calibration Chart for Accelerometer Type 4371 V.
[9] P. Berthoud and T. Baumberger, Proc. R. Soc. London Ser. A (in press).